



Original Article

Molecular cloning and characterization of the INK4a and ARF genes in naked mole-rat

Shingo Miyawaki^{1,2)}, Yoshimi Kawamura¹⁾, Tsuyoshi Hachiya³⁾,
Atsushi Shimizu³⁾ and Kyoko Miura^{1,2,*}

¹⁾Biomedical Animal Research Laboratory, Institute for Genetic Medicine, Hokkaido University, Hokkaido, Japan

²⁾Department of Physiology, Keio University School of Medicine, Tokyo, Japan

³⁾Iwate Tohoku Medical Megabank Organization Iwate Medical University, Iwate, Japan

The naked mole-rat (NMR) is the world's longest-living rodent, with a maximum lifespan of longer than 31 years without any evidence of neoplastic disease. Recently, the NMR has come to be regarded as a useful animal model for the study of longevity and cancer resistance. Sequencing analysis of the NMR genome revealed the existence of species-specific changes in the predicted sequence of the INK4a and ARF tumor suppressors, suggesting the possibility that these two genes might have important roles in NMR's unique longevity and cancer resistance. Here, we report the molecular cloning and characterization of the INK4a and ARF genes *in vitro*. To investigate the expression and function of the INK4a and ARF genes in NMR, we generated several research tools, including antibodies, real-time PCR primer sets, and overexpression and knockdown vectors. Our results showed that endogenous expression of INK4a and ARF was upregulated in NMR fibroblasts treated with DNA-damaging agents or after serial passaging. In addition, overexpression of INK4a or ARF caused cell cycle arrest in both NMR fibroblasts and mouse NIH-3T3 cells. These results suggest INK4a and ARF execute a conserved function as cell cycle inhibitors in NMR. The research tools developed in the present study will be useful for exploring the specific function of INK4a and ARF genes in the unique longevity and cancer-resistant phenotype of NMRs.

Rec.12/15/2014, Acc.12/21/2014, pp42-50

*Correspondence should be addressed to:

Kyoko Miura, PhD, Biomedical Animal Research Laboratory, Institute for Genetic Medicine, Hokkaido University, Kita-15 Nishi-7, Kita-ku, Sapporo 060-0815, Japan. Phone: +81-11-706-6053, Fax: +81-11-706-6053, E-mail: miura@igm.hokudai.ac.jp

Key words

ARF, cell cycle, INK4a, naked mole rat

Introduction

The naked mole-rat (NMR, *heterocephalus glaber*) is a small, nearly hairless rodent (average body weight of

around 30 g in our captive colony) found in the horn of Africa, primarily in Ethiopia, Kenya, and Somalia¹⁾. NMRs live underground in colonies typically comprised of 60-80



individuals. Interestingly, the NMR is one of two unique mammals that have a eusocial hierarchy comparable to ants and bees², in which only one breeding female and one to three breeding males play a reproductive role in the colony^{2, 3}. NMRs are also famous for their unique poikilothermic phenotype, with a low body temperature (32°C)^{4, 5}. Recently, NMR has received worldwide attention for its extraordinary longevity and cancer-resistant phenotype. NMR's maximum life span exceeds 31 years in captivity and is considered to show a negligible senescence phenotype^{3, 6}. They show no age-related decline in body composition or physiological function, including fecundity, for over 75% of their lifespan. Moreover, spontaneous neoplasm in NMRs has never been observed^{3, 7}.

Recently, some reports have proposed possible mechanisms that may contribute to NMR's cancer resistance and longevity. Perez et al. showed that protein stability in NMRs is high in spite of certain accumulation of oxidative stress during aging⁸. One cancer-resistant mechanism, a unique contact inhibition system termed "early contact inhibition", is proposed to occur only in NMR fibroblasts⁹. NMR adult fibroblasts stop proliferation upon the formation of cell-cell contacts. Recently, Tian et al. showed that high molecular weight hyaluronan mediates early contact inhibition and resistance to cellular transformation in NMR fibroblasts¹⁰. However, the primary mechanism responsible for NMR's extraordinary cancer resistance and longevity remains unknown.

Since the NMR genome sequence was reported in 2011, several NMR-specific coding sequences possibly contributing to the longevity and cancer resistance of NMRs have been reported¹¹⁻¹³. Notably, Kim et al. demonstrated that the predicted sequences of the potent tumor suppressors INK4a and Alternative reading frame (ARF) contain species-specific changes in NMRs. They identified two early stop codons in the second exon of INK4a and four early stop codons in the second exon of ARF that result in the translation of truncated INK4a and ARF proteins¹¹. Moreover, Seluanov et al. reported that the expression of INK4a is associated with early contact inhibition⁹.

INK4a and ARF genes are potent tumor suppressors sharing two exons encoded in the CDKN2a gene locus¹⁴⁻¹⁷. INK4a and ARF activate two crucial tumor suppressor pathways, the Retinoblastoma protein (Rb) and p53 pathways, respectively. INK4a binds to cyclin dependent kinase (CDK) 4/6 and inhibits its function, which in turn activates Rb¹⁴. ARF activates p53 by binding to and

inhibiting Mdm2, a destabilizer of p53¹⁸. The activation of these pathways prevents aberrant cell growth by inducing apoptosis or cellular senescence¹⁹⁻²¹. Overexpression of ARF causes cell cycle arrest in NIH-3T3 cells²², and mice that lack either INK4a or ARF exhibit a tumor-prone phenotype^{17, 23, 24}. INK4a and ARF genes are also known as biomarkers of aging. In several rodents and human, expression of INK4a and ARF is elevated in several tissues during aging²⁵. Interestingly, Baker et al. recently revealed that the depletion of INK4a-expressing cells can attenuate the aging phenotype in BubR1 progeroid mice²⁶. Thus, INK4a and ARF genes play a critical role in aging and protection from cancer.

From the above reports, it can be postulated that the sequence changes in these genes in NMR might play an important role in their cancer-resistant and longevity phenotypes. Although Keane et al. predicted the exon-intron structure and coding sequence of the NMR INK4a gene based on their assembled sequence data and an *in silico* method¹³, no one has definitively reported the coding sequence of the NMR INK4a and ARF genes as determined by cloning and Sanger sequencing experiments. Prior to study of the biological function of INK4a and ARF genes in NMR, some basic information and research tools needed to be established. First, cloning and Sanger sequencing of the NMR INK4a and ARF coding sequences were essential. Next, antibodies that detect NMR INK4a and ARF proteins were required for expression analyses. It was also important to construct vectors for overexpression or knockdown experiments.

Here, we report the molecular cloning and characterization of NMR INK4a and ARF genes. We cloned the INK4a and ARF coding sequences from cultured cells and introduced them into lentiviral expression vectors. We also generated rabbit polyclonal antibodies that detect INK4a or ARF proteins of NMR, but not those of mouse. Finally, we revealed the conserved function of INK4a and ARF genes as cell cycle inhibitors in NMR cell culture and lack of their ability to lead cell death in NIH-3T3 cells.

Materials and Method

1) Animals and cell culture

Primary NMR skin fibroblasts were obtained from adult female (60 months) and male (14 months) NMRs maintained at Keio University. Animals were euthanized via isoflurane through a nose cone and biopsies of subcutaneous tissue were taken. These tissues were



minced and enzymatically digested with 0.25% trypsin and 0.2% collagenase. The digested samples were then neutralized and cultured in Dulbecco's Modified Eagle's Medium (DMEM: Sigma) supplemented with 15% fetal bovine serum (FBS: BioWest), nonessential amino acids (NEAA; Sigma), 2% L-glutamine (L-glu; Sigma) and 1% penicillin/streptomycin (P/S: Sigma) under an atmosphere of humidified 5% CO₂ and 5% O₂ at 32°C. The medium was changed every 2 days and the cells were passaged every 5 days. In this study, all primary NMR fibroblasts were used at passage 3-6. 293T cells were cultured in DMEM supplemented with 10% FBS, 2% NEAA, 2% L-glu, and 1% P/S and incubated at 5% CO₂ at 37°C. NIH-3T3 cells were cultured in DMEM supplemented with 10% cow serum, 2% NEAA, 2% L-glu and 1% P/S and plated on gelatin-coated dish. All the experimental procedures were approved by the Ethics Committee of Keio University (12024-(0)) and Hokkaido University (14-0065) and were conducted in accordance with the Guide for the Care and Use of Laboratory Animals (US National Institutes of Health).

2) Cloning of NMR INK4a and NMR ARF coding sequences

Total RNA was purified with Trizol reagent (Invitrogen) from NMR fibroblasts. Reverse transcription of 500 ng total RNA with ReverTra Ace (Toyobo, Japan) was performed according to the manufacturer's instructions. Polymerase chain reaction (PCR) was performed using the primers shown in Table 1. These primers were designed based on cDNA sequences obtained from BGI deposited genome information¹⁰. The cDNA fragments were inserted into the pENTR/D-TOPO entry vector plasmid and verified by Sanger sequencing.

3) Generation of rabbit polyclonal antibodies that react with NMR INK4a or ARF

Rabbit polyclonal anti-NMR INK4a antibody and anti-NMR ARF antibody were generated against sequences of the respective synthesized peptide. The epitope of the anti-NMR INK4a antibody was three partially synthesized peptides, and the epitope of NMR ARF was a single synthesized peptide. (Medical and Biological Laboratories Co., Ltd., Nagoya, Japan). The peptide sequences used as antibody epitopes are shown in Table 1.

4) Western blotting analysis

The cells were washed with PBS, lysed in cell lysis buffer

Table 1 Primer sequence, Epitope sequence and Knock down vector sequence

Gene	Primer sequence
NMR-ARF	F 5'-GCG TGG TCC TGG TCC GCA CT-3'
	R 5'-ATC TCT GAA TTA TCC GTC CTC ACC T-3'
NMR-ARF-RT	F 5'-CCA TCG TGT GTG CCG GCT TTC GT-3'
	R 5'-CTG CTG CCC TCT CCG GTG TCT-3'
NMR-INK4a-RT	F 5'-GAC CCG AAC TGC GCT GAC CCT-3'
	R 5'-CCG CGT CAT GCA CCG GTA GTG TGA-3'
antibody	Epitope sequence
anti-ARF	RPGHDDGQHPSGRAAC (66-80)
	CQGHREVARYLRDVVGDV (113-129)
	MDSWGEKLATAAARC (1-14)
	CRELLEAGAPPNARNR (21-35)
Target gene	Target sequence (DNA)
shINK4a-1	5'-GGTCCAGGAGGTACGCGAGCT-3'
shINK4a-2	5'-GCCAATGCCCGGAACCGTTT-3'
shARF-1	5'-GGCCCTCTTGCTGATGCTAGT-3'
shARF-2	5'-GGGCTTTCGTGGTGCAGATCC-3'
shCDKN2a-1	5'-GATGATGGGCAACACCCAAGT-3'
shCDKN2a-2	5'-GCTTCTTGATACTCTGGTGG-3'

(62.5 mM Tris-HCl, pH 6.8, containing 2% SDS and 5% sucrose) and boiled for 10 min. Protein concentrations were measured using a Pierce BCA Protein Assay Kit. The samples (293T cells: 5 µg, NMR fibroblasts: 10 µg) were subjected to SDS-PAGE, and the separated proteins were transferred to a PVDF membrane using a Trans-Blot Turbo Transfer System (Bio-Rad). Membranes were probed with antibodies against NMR INK4a (original antibody) at 1:1,000, NMR ARF (original antibody) at 1:1,000 and β-actin (Sigma) at 1:10,000. The membranes were incubated with horseradish peroxidase-conjugated anti-rabbit or anti-mouse IgG secondary antibodies (Cell Signaling Technology) and visualized using enhanced chemiluminescence (ECL; GE Healthcare).

5) Immunocytochemical analysis

293T cells overexpressing NMR-INK4a and NMR-ARF were fixed with 4% paraformaldehyde in PBS for 5 min and then treated with 0.3% Triton X-100 and Tris-NaCl-blocking buffer (TNB; PerkinElmer) for 60 min at room temperature. The primary antibodies, anti-NMR INK4a (Rabbit IgG, 1:1000), anti-NMR ARF (rabbit IgG, 1:1000), and anti-γH2AX (mouse monoclonal clone JBW301; Millipore 1:1000) were diluted with 0.3% Triton X-100 and TNB and incubated for 24 h at 4°C. The cells were then incubated with secondary antibody (1:1000, Alexa 555 mouse IgG) and 1 µg/ml Hoechst 33342 for nuclei staining for 60 min at room temperature.



6) RNA isolation and quantitative RT-PCR

Runs were performed on a StepOne Real-Time PCR System (Applied Biosystems) using Fast SYBR® Green Master Mix (Applied Biosystems). Primer sequences are shown in Table 1.

7) Cellular senescence assay

Cellular senescence was induced by treating the cells with 200 nM of mitomycin C for 24 hours twice. SA-βgal staining was performed using senescence detection kit (BioVision) according to the manufacture's instruction.

8) Cell cycle analysis

Cells were trypsinized, washed twice with PBS, and fixed in ice-cold 70% ethanol for 2 h. Subsequently, cells were stained with propidium iodide and subjected to flow cytometric analysis based on DNA content. The samples were then analyzed for cell cycle distribution using a FACS Calibur (Becton-Dickinson) and the Dean-Jett-Fox algorithm in FlowJo software (Treestar).

9) Lentivirus preparation

Lentiviruses were produced by transient transfection of 293T cells with pCSII-EF-NMR-INK4a-TK-hyg, pCSII-EF-NMR-ARF-TK-hyg or pCSII-EF-Ms-Arf-TK-hyg plasmids and lentivirus constructs pCMV-VSV-G-RSV-Rev and pCAG-HIVgp²⁷ using Gene Juice transfection reagent (Novagen) according to the manufacturer's instructions. The conditioned medium containing virus particles was concentrated and used for viral transduction.

10) Trypan Blue Exclusion Test

To determine the number of viable or dead cells, cell suspension was stained with trypan blue and the stained cells were counted as dead cells.

11) Statistical analysis

Student's *t*-tests (two-tailed) were used for the statistical analysis of differences between two groups. All data are presented as the means ± s.d. from three biological replicates.

Results

1) Cloning of INK4a and ARF genes of NMR

To confirm the previously predicted coding sequences of INK4a and ARF in NMR^{11, 13}, we performed cDNA cloning of INK4a and ARF coding sequences from a skin fibroblast

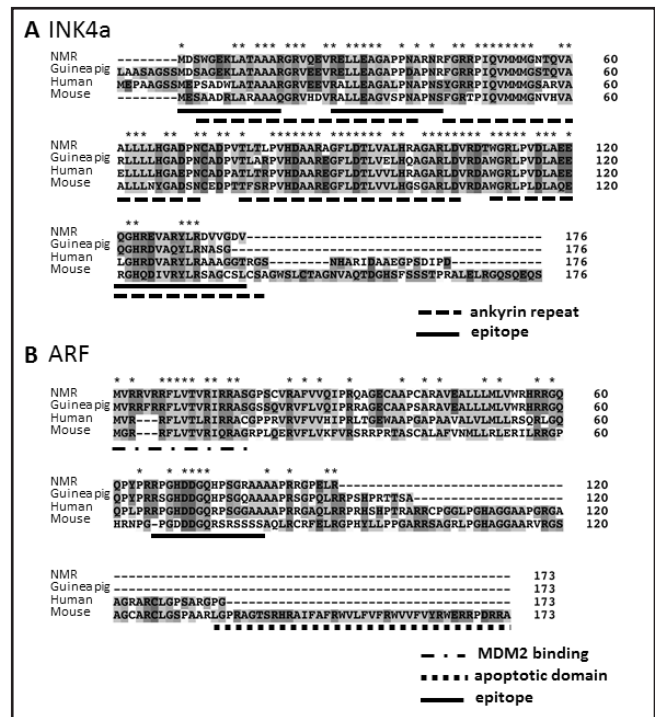


Fig. 1 Sequence comparison of naked mole-rat, guinea pig, human and mouse INK4a/ARF

Asterisks indicate the same sequence in the four species. NMR sequences were obtained from NMR skin fibroblast cDNA. (A)The amino acid sequence of INK4a in NMR is most similar to that of guinea pig. The feature of INK4a within four ankyrin repeats sequences were shown. (B)The amino acid sequence of ARF in NMR is the shortest of the four species. The region of MDM2 binding site and mouse apoptotic domain were shown. The stars indicate the residues conserved in all species. The black bars indicate the epitope of anti- INK4a and -ARF antibody.

cDNA library. First, we retrieved sequence information from around the INK4a/ARF locus from scaffold 173 in the BGI genome database¹¹. Next, we performed cloning and Sanger sequencing of DNA fragments containing full-length of INK4a or ARF coding sequences from skin fibroblasts. The resulting sequences of cloned INK4a and ARF were identical to the predicted sequences reported previously. The sequence of NMR ARF was deposited in GenBank (accession number: LC012308). We next compared the amino acid sequences of these genes with those of guinea pig, human, and mouse found in the NCBI database (Figs. 1A and 1B). As reported previously, the amino acid sequences of INK4a and ARF in NMR were truncated forms. We found that the amino acid sequences in guinea pig were also truncated for both INK4a, as reported previously¹¹, as well as ARF. The four ankyrin repeat sequences and threonine residue important for CDK6

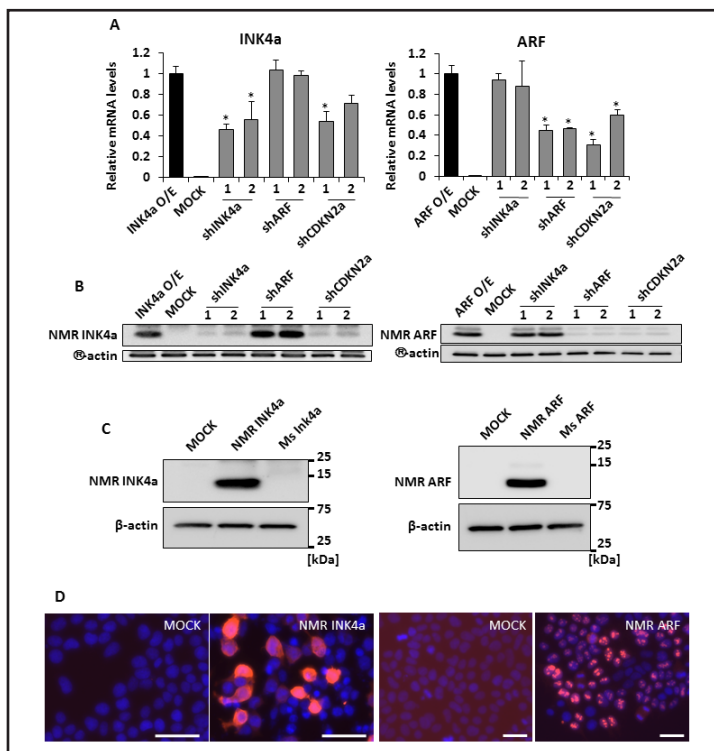


Fig.2 Generation and evaluation of INK4a/ARF over-expressing/knockdown vectors and antibodies

shRNAs targeting INK4a, ARF, and common sequences in these genes were transfected into INK4a- or ARF-expressing 293T cells. Real-time PCR and western blotting were performed to evaluate the antibodies generated against NMR INK4a and ARF, and the efficiency of the knockdown vectors. (A)Relative expression of INK4a or ARF. All values were normalized to β -actin. (B)Protein levels of INK4a and ARF were analyzed by western blot. β -actin was used as a loading control. (C)The molecular weight of the NMR INK4a and ARF were showed and the antibodies did not detect the Ink4a and ARF protein of mouse. (D)Immunocytochemistry of NMR INK4a and NMR ARF when overexpressed in 293T cells. Nuclei (blue) were stained with Hoechst 33342. Scale bar represents 100 μ m. O/E represents over expression.

binding were conserved in NMR INK4a, suggesting that the role of INK4a in cell cycle arrest is preserved in NMR. Amino acid sequence analysis of NMR ARF showed that it is shorter than ARF in mouse, human, and guinea pig, due to the early stop codon at amino acid 91. A notable change in NMR ARF was loss of the p53-independent apoptosis domain in the carboxy-terminus (amino acids 130-169) of ARF, which is also missing in human ARF.

2)Generation and evaluation of overexpression/knockdown vectors and antibodies against NMR INK4a and ARF

Because both NMR INK4A and ARF have unique amino acid sequences, we generated rabbit polyclonal antibodies and real-time PCR primer sets able to detect INK4a and ARF protein and mRNA expression, respectively (Table 1). In addition, NMR INK4a or ARF were introduced into lentiviral overexpression vectors²⁷. Finally, we generated knockdown vectors expressing shRNAs that bind specifically to INK4a and ARF or exon2 of CDKN2a, which is shared by these two genes. The target sequences of shRNAs are shown in Table 1. The shRNAs against INK4a, ARF and CDKN2a were then transfected into NMR INK4a- or NMR ARF-expressing 293T cells, and real-time PCR and western blotting were performed to evaluate the knockdown

efficiency. PCR results confirmed that the expression of INK4a, ARF, or both were repressed at the mRNA level by each knockdown vector (Fig. 2A), and western blotting revealed that the newly generated antibodies could clearly detect the ectopically expressed INK4a and ARF proteins (Fig. 2B). We also found that the expression of INK4a, ARF, or both was successfully repressed by transduction of each shRNA knockdown vectors. Using these antibodies, we then determined the molecular weight of NMR INK4a and ARF. The molecular weight of NMR INK4a was 14 kDa, in agreement with its predicted size. We also detected an obvious band near the 10 kDa at the predicted size of NMR ARF (Fig. 2C). Immunocytochemistry performed using these antibodies consistently detected NMR INK4a in the cytoplasm and nuclear compartment, while NMR ARF was localized to the nucleoli (Fig. 2D).

3)Elevation of endogenous INK4a and ARF expression levels during cellular senescence in NMR fibroblasts

INK4a and ARF genes are well known as cellular senescence markers^{21, 28}. To determine whether INK4a and ARF are upregulated after induction of cellular senescence in adult NMR fibroblasts by treatment with the DNA-damaging agent, mitomycin C (MMC), or serial passage, we performed real-time PCR analysis and western blotting. MMC-treated

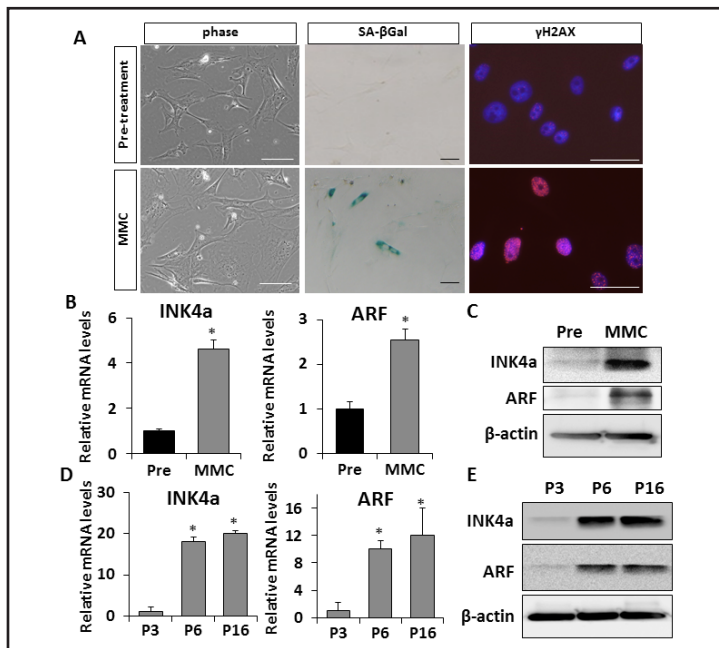


Fig.3 Upregulation of INK4a and ARF expression by induction of cellular senescence in NMR fibroblasts

(A) Cellular senescence was induced using mitomycin C (MMC) treatment. MMC-treated NMR fibroblasts show a typical senescence-like morphology. Histochemical staining of MMC-treated cells for SA-β-gal activity. The staining of γH2AX foci. Nuclei (blue) were stained with Hoechst 33342. (B) The mRNA expression of INK4a and ARF. (C) Protein levels of INK4a and ARF were analyzed by western blot. β-actin was used as a loading control. Both genes were upregulated after induction of senescence. (D) Real-time PCR analysis of serially-passaged NMR fibroblasts. (E) Western blot analysis of serially-passaged NMR fibroblasts. Scale bar represents 100 μm.

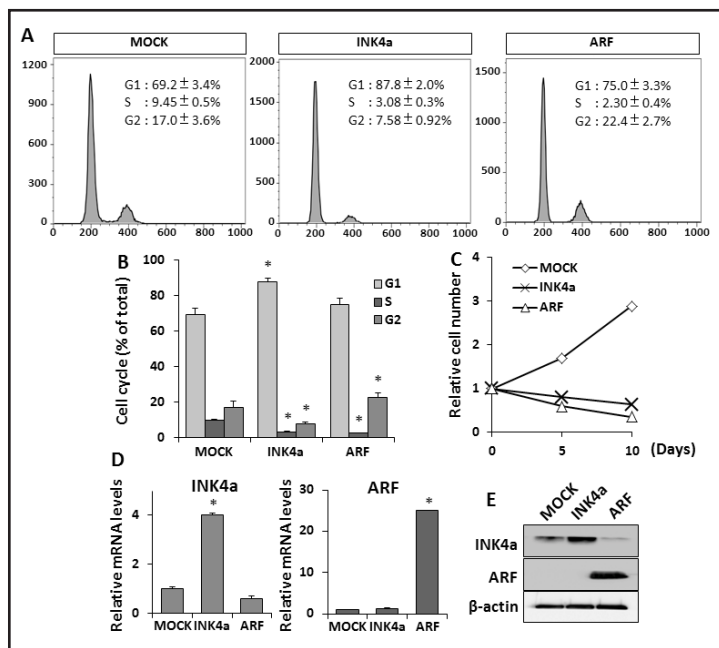


Fig.4 The effect of ectopic expression of INK4a and ARF on cell cycle properties

(A and B) NMR skin fibroblasts were infected with lentiviruses encoding NMR INK4a, NMR ARF, or EGFP. Seven days after infection, cell cycle analysis was performed by flow cytometry using a FACS Calibur (Becton-Dickinson) and the Dean-Jett-Fox algorithm in FlowJo software. (C) Proliferation of INK4a- or ARF-expressing NMR fibroblasts. Cells were plated at an initial density of 2.5×10^5 and counted after 5 days. (D) Relative expression of INK4a or ARF. All values were normalized to β-actin. (E) Protein levels of INK4a and ARF were analyzed by western blot. β-actin was used as a loading control.

NMR fibroblasts showed a large, flat morphology, similar to that of senescent cells (Fig. 3A). SA-β-gal-positive cells in NMR fibroblasts were also increased after MMC treatment (Fig. 3A), indicating the induction of cellular senescence. MMC treated NMR fibroblasts were found to accrue considerable DNA damage as shown by the accumulation and the increase in the intensity of γH2AX foci, a marker of DNA damage (Fig. 3A). As shown in Figures 3B and 3C, expression of INK4a and ARF was increased at both the message and protein levels after induction of cellular

senescence. Likewise, the serially-passaged NMR fibroblasts also expressed INK4a and ARF (Figs. 3D and 3E).

4) NMR INK4a and ARF genes have the potential to induce G1 and G2 cell cycle arrest

Finally, to evaluate whether NMR INK4a and ARF inhibit cell cycle progression, as in other species, we used lentiviral expression vectors to overexpress NMR INK4a or ARF in NMR skin fibroblasts. Ectopic expression of NMR INK4a or ARF was confirmed at both the mRNA and protein

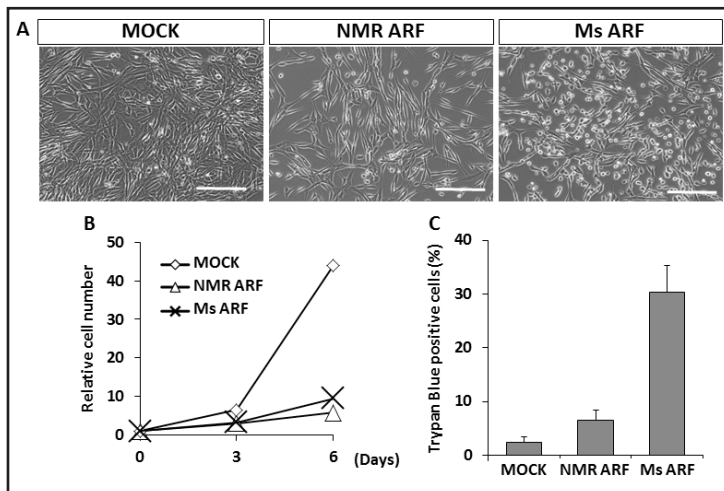


Fig.5 The cell death-inducing ability of NMR ARF is attenuated compared to that of Ms ARF

(A)The morphology of NMR ARF or Ms ARF overexpressed NIH-3T3 cells. Scale bar represents 200 μm . (B)Analysis of Cell Growth. Cells were seeded at 5×10^5 cells per 100-mm dish, and the cells were passaged and counted every 3 days. (C)The population of cell death was counted by trypan blue exclusion methods.

levels (Figs. 4D and 4E). NMR fibroblasts overexpressing each gene stopped proliferating (Fig. 4C). Flow cytometric analysis following DNA staining by propidium iodide revealed an increase in the percentage of cells in G1 phase and a decrease in the percentage of cells in S phase in NMR INK4a-expressing cells (Figs. 4A and 4B). NMR ARF-expressing cells showed G2 arrest, but no significant increase in the G1 population. Thus, NMR INK4a and ARF have the potential to inhibit the cell cycle at the G1 or G2 phase, as in mouse and human¹⁸.

5)The cell-death-inducing ability of NMR ARF is attenuated compared to that of Ms ARF in NIH-3T3 cells

To evaluate the cell death inducing function of NMR ARF, which does not have the p53-independent apoptosis domain in carboxy-terminus (amino acids sequence of 130-169), we introduced NMR ARF or Ms ARF into NIH-3T3 cells. As a result, over expression of both NMR ARF and Ms ARF induced cell growth inhibition (Figs. 5A and B). The cell death population was calculated by trypan blue exclusion test and we found that an obvious cell death was induced in NIH-3T3 cells by ectopic expression of Ms ARF. In contrast, the ectopic expression of NMR ARF did not induce significant cell death (Fig. 5C), indicating that the deficiency of C-terminus apoptotic domain in NMR ARF results in a reduction of activate cell death.

Discussion

In this study, we cloned the NMR INK4a and ARF coding sequences and submitted the NMR ARF sequences to the GenBank repository. The sequences of the cloned INK4a and ARF genes are identical to those in the recently

reported BGI genome sequence¹¹. We found that both NMR INK4a and ARF contain early stop codons, resulting in the expression of shorter forms of the proteins compared to INK4a and ARF in human or mouse. We also developed basic research tools, including antibodies, real-time PCR primer sets, and overexpressing and knockdown vectors to carry out several biological analyses of NMR INK4a and ARF. We detected the upregulation of endogenous mRNA and protein expression following the induction of cellular senescence, and showed that NMR INK4a and ARF exhibit cell cycle inhibiting activity.

To date, little information on the biological roles of INK4a and ARF in NMR was available due to the difficulty in detecting NMR INK4a and ARF transcript and protein. The C-terminus truncations in NMR INK4a and ARF preclude the use of commercially available antibodies targeted to INK4a and ARF of human or mouse. Furthermore, since these genes share the same exon sequences, strict specificity is required to detect each gene, even at the RNA level. To address this issue in the present study, we developed several tools for investigating the expression and function of NMR INK4a and ARF, including antibody and primer sets to detect NMR INK4a and ARF specifically.

We revealed that NMR INK4a and ARF expression was upregulated at both the mRNA and protein level after the induction of senescence in NMR fibroblasts, just as in mouse. INK4a and ARF are known to be expressed at very low levels in most tissues in young organisms, but become de-repressed during aging²⁹. Our studies will allow us to use INK4a and ARF as molecular markers of cellular senescence and aging in NMRs.

Subsequently, we found that the overexpression of NMR



INK4a or ARF have the potential to induce G1 and G2 cell cycle arrest in NMR fibroblasts, similar to their role in human and mouse^{18, 30}. As reported previously, guinea pig INK4a is of similar length as INK4a in NMR and shorter than in human and mouse; thus, the truncation of INK4a is not an NMR-specific adaptation. This observation suggests that the function of INK4a is highly preserved in NMR¹³. In the case of ARF, various studies have proposed that the N-terminus region of ARF is the region primarily responsible for its tumor-suppressing activities. This region is relatively well conserved between NMR, guinea pig, human, and mouse³¹, indicating that tumor suppressive activity through activation of the p53 pathway would be conserved in NMR ARF. In this region, ARF in NMR and guinea pig have a three amino acid residue insertion (amino acids 4-6), including two basic arginine residues. This observation raises the possibility that altered MDM2 binding affinity would make the tumor-suppressing function of p53 pathway more active in NMR and guinea pig. Interestingly, the NMR-ARF did not contain the C-terminus apoptosis domain found in the mouse ARF amino acid sequence³¹. Based on the percentages of apoptotic cells in NIH-3T3 cells overexpressing either NMR ARF or Ms ARF, it appears that the cell-death-inducing activity of NMR ARF is attenuated compared to Ms ARF.

In conclusion, we experimentally investigated the core function of INK4a and ARF genes in NMR, previously predicted to have conserved function based on sequencing homology. Our results showed that the function of the NMR INK4a and ARF genes in inhibiting cell cycle progression and exhibiting elevated expression during cellular senescence resembled that of mouse and human. The shorter forms of INK4a and ARF would affect other features of NMR INK4a and ARF, such as protein stability, polarity, and activity. Further study will be required to identify the specific function of NMR INK4a and ARF. The research tools developed in the present study will be useful for investigating further the function of INK4a and ARF in the NMR cancer resistance and longevity phenotypes.

Acknowledgement and Source of funding

We sincerely and deeply thank Dr. Hideyuki Okano and the colleagues in Okano laboratory for help, encouragement and advice.

This work was supported by grants from the Ministry of Education, Culture, Sports, Science and Technology of Japan, Takeda Science Foundation, Japanese Foundation For Aging and Health. K.M. is supported by the Japan Science and Technology Agency (PRESTO).

S.M. is supported by Research Fellowships for Young Scientists from Japan Society for the Promotion of Science (JSPS).

Conflict of interests

The authors declare no competing financial interests.

References

- 1) Lavocat R: Evolution of African Mammals. Harvard University Press, Cambridge, UK, 1978. pp68-89.
- 2) Jarvis JU: Eusociality in a mammal: cooperative breeding in naked mole-rat colonies. *Science*. 1981; 212: 571-573.
- 3) Buffenstein R: Negligible senescence in the longest living rodent, the naked mole-rat: insights from a successfully aging species. *J Comp Physiol B*. 2008; 178: 439-445.
- 4) Buffenstein R, Woodley R, Thomadakis C, Daly TJ, Gray DA: Cold-induced changes in thyroid function in a poikilothermic mammal, the naked mole-rat. *Am J Physiol Regul Integr Comp Physiol*. 2001; 280: 149-155.
- 5) Woodley R, Buffenstein R: Thermogenic changes with chronic cold exposure in the naked mole-rat (*Heterocephalus glaber*). *Comp Biochem Physiol A Mol Integr Physiol*. 2002; 133: 827-834.
- 6) Grimes KM, Reddy AK, Lindsey ML, Buffenstein R: And the beat goes on: maintained cardiovascular function during aging in the longest-lived rodent, the naked mole-rat. *Am J Physiol Heart Circ Physiol*. 2014; 307: 284-291.
- 7) Edrey YH, Hanes M, Pinto M, Mele J, Buffenstein R: Successful aging and sustained good health in the naked mole rat: a long-lived mammalian model for biogerontology and biomedical research. *ILAR J*. 2011; 52: 41-53.
- 8) Pérez VI, Buffenstein R, Masamsetti V, Leonard S, Salmon AB, Mele J, Andziak B, Yang T, Edrey Y, Friguet B, Ward W, Richardson A, Chaudhuri A: Protein stability and resistance to oxidative stress are determinants of longevity in the longest-living rodent, the naked mole-rat. *Proc Natl Acad Sci U S A*. 2009; 106: 3059-3064.
- 9) Seluanov A, Hine C, Azpurua J, Feigenson M, Bozzella M, Mao Z, Catania KC, Gorbunova V: Hypersensitivity to contact inhibition provides a clue to cancer resistance of naked mole-rat. *Proc Natl Acad Sci U S A*. 2009; 106: 19352-19357.
- 10) Tian X, Azpurua J, Hine C, Vaidya A, Myakishev-Rempel M, Ablaeva J, Mao Z, Nevo E, Gorbunova V,



- Seluanov A: High-molecular-mass hyaluronan mediates the cancer resistance of the naked mole rat. *Nature*. 2013; 499: 346-349.
- 11) Kim EB, Fang X, Fushan AA, Huang Z, Lobanov AV, Han L, Marino SM, Sun X, Turanov AA, Yang P, Yim SH, Zhao X, Kasaikina MV, Stoletzki N, Peng C, Polak P, Xiong Z, Kiezun A, Zhu Y, Chen Y, Kryukov GV, Zhang Q, Peshkin L, Yang L, Bronson RT, Buffenstein R, Wang B, Han C, Li Q, Chen L, Zhao W, Sunyaev SR, Park TJ, Zhang G, Wang J, Gladyshev VN: Genome sequencing reveals insights into physiology and longevity of the naked mole rat. *Nature*. 2011; 479: 223-227.
- 12) Fang X, Seim I, Huang Z, Gerashchenko MV, Xiong Z, Turanov AA, Zhu Y, Lobanov AV, Fan D, Yim SH, Yao X, Ma S, Yang L, Lee SG, Kim EB, Bronson RT, Šumbera R, Buffenstein R, Zhou X, Krogh A, Park TJ, Zhang G, Wang J, Gladyshev VN: Adaptations to a subterranean environment and longevity revealed by the analysis of mole rat genomes. *Cell Rep*. 2014; 8: 1354-1364.
- 13) Keane M, Craig T, Alföldi J, Berlin AM, Johnson J, Seluanov A, Gorbunova V, Di Palma F, Lindblad-Toh K, Church GM, de Magalhães JP: The Naked Mole Rat Genome Resource: facilitating analyses of cancer and longevity-related adaptations. *Bioinformatics*. 2014; 30: 3558-3560.
- 14) Serrano M, Hannon GJ, Beach DA: new regulatory motif in cell-cycle control causing specific inhibition of cyclin D/CDK4. *Nature*. 1993; 366: 704-707.
- 15) Hannon GJ, Beach D: p16INK4B is a potential effector of TGF-beta-induced cell cycle arrest. *Nature*. 1994; 371: 257-261.
- 16) Duro D, Flexor MA, Bernard O, d'Agay MF, Berger R, Larsen CJ: Alterations of the putative tumor suppressor gene p16/MTS1 in human hematological malignancies. *C R Acad Sci III*. 1994; 317: 913-919.
- 17) Kamijo T, Zindy F, Roussel MF, Quelle DE, Downing JR, Ashmun RA, Grosveld G, Sherr CJ: Tumor suppression at the mouse INK4a locus mediated by the alternative reading frame product p19ARF. *Cell*. 1997; 91: 649-659.
- 18) Quelle DE, Zindy F, Ashmun RA, Sherr CJ: Alternative reading frames of the INK4a tumor suppressor gene encode two unrelated proteins capable of inducing cell cycle arrest. *Cell*. 1995; 15: 993-1000.
- 19) Serrano M, Lin AW, McCurrach ME, Beach D, Lowe SW: Oncogenic ras provokes premature cell senescence associated with accumulation of p53 and p16INK4a. *Cell*. 1997; 88: 593-602.
- 20) Gil J, Peters G: Regulation of the INK4b-ARF-INK4a tumour suppressor locus: all for one or one for all. *Nat Rev Mol Cell Biol*. 2006; 7: 667-677.
- 21) Collado M, Blasco MA, Serrano M: Cellular senescence in cancer and aging. *Cell*. 2007; 130: 223-233.
- 22) Quelle DE, Zindy F, Ashmun RA, Sherr CJ: Alternative reading frames of the INK4a tumor suppressor gene encode two unrelated proteins capable of inducing cell cycle arrest. *Cell*. 1995; 15: 993-1000.
- 23) Serrano M, Lee H, Chin L, Cordon-Cardo C, Beach D, DePinho RA: Role of the INK4a locus in tumor suppression and cell mortality. *Cell*. 1996; 85: 27-37.
- 24) Krimpenfort P, Quon KC, Mooi WJ, Loonstra A, Berns A: Loss of p16Ink4a confers susceptibility to metastatic melanoma in mice. *Nature*. 2001; 413: 83-86.
- 25) Krishnamurthy J, Ramsey MR, Ligon KL, Torrice C, Koh A, Bonner-Weir S, Sharpless NE: p16INK4a induces an age-dependent decline in islet regenerative potential. *Nature*. 2006; 443: 453-457.
- 26) Baker DJ, Wijshake T, Tchkonja T, LeBrasseur NK, Childs BG, van de Sluis B, Kirkland JL, van Deursen JM: Clearance of p16Ink4a-positive senescent cells delays ageing-associated disorders. *Nature*. 2011; 479: 232-236.
- 27) Miyoshi H, Blomer U, Takahashi M, Gage FH, Verma IM: Development of a self-inactivating lentivirus vector. *J Virol*. 1998; 72: 8150-8157.
- 28) Sherr CJ: The INK4a/ARF network in tumour suppression. *Nature reviews*. *Nat Rev Mol Cell Biol*. 2001; 2: 731-737.
- 29) Krishnamurthy J, Torrice C, Ramsey MR, Kovalev GI, Al-Regaiey K, Su L, Sharpless NE: Ink4a/Arf expression is a biomarker of aging. *J Clin Invest*. 2004; 114: 1299-1307.
- 30) Quelle DE, Cheng M, Ashmun RA, Sherr CJ: Cancer-associated mutations at the INK4a locus cancel cell cycle arrest by p16INK4a but not by the alternative reading frame protein p19ARF. *Proc Natl Acad Sci U S A*. 1997; 94: 669-673.
- 31) Matsuoka M, Kurita M, Sudo H, Mizumoto K, Nishimoto I, Ogata E: Multiple domains of the mouse p19ARF tumor suppressor are involved in p53-independent apoptosis. *Biochem Biophys Res Commun*. 2003; 301: 1000-1010.